Limnol. Oceanogr., 58(6), 2013, 2101–2108

doi:10.4319/lo.2013.58.6.2101

Mats of the nonnative macroalga, *Gracilaria vermiculophylla*, alter net denitrification rates and nutrient fluxes on intertidal mudflats

Dana J. Gonzalez,[1,*] Ashley R. Smyth,[2] Michael F. Piehler,[2] and Karen J. McGlathery[1]

[1] Department of Environmental Sciences, University of Virginia, Charlottesville, Virginia
[2] The University of North Carolina at Chapel Hill, Institute of Marine Sciences, Morehead City, North Carolina

Abstract

We hypothesized that mats of a nonnative macroalga, *Gracilaria vermiculophylla*, which is often found incorporated several centimeters into intertidal mudflat sediments, would increase net denitrification rates relative to bare sediments. At moderate densities (~ 40 g dry weight [dry wt] m^{-2}), net denitrification rates in June (182.37 ± 16.87 μmol N-N_2 m^{-2} h^{-1}), July (213.19 ± 16.30 μmol N-N_2 m^{-2} h^{-1}), and September (124.82 ± 11.17 μmol N-N_2 m^{-2} h^{-1}) were higher than rates previously documented with macroalgal mats. Compared with rates from bare sediment in June (25.48 ± 15.09 μmol N-N_2 m^{-2} h^{-1}) and September (46.47 ± 15.79 μmol N-N_2 m^{-2} h^{-1}), net denitrification was significantly higher when *G. vermiculophylla* was present. Rates measured on bare sediment in July (254.81 ± 19.86 μmol N-N_2 m^{-2} h^{-1}) were not significantly different from *G. vermiculophylla* counterparts, most likely because of highly reduced conditions in *G. vermiculophylla* cores, which could have limited nitrification. July incubations also demonstrate that at higher densities (~ 120 g dry wt m^{-2} *G. vermiculophylla*), denitrification rates can drop, suggesting a potential biomass threshold for macroalgal enhancement of denitrification.

Human interactions with the environment, including the introduction of nonnative species and alterations to nutrient regimes, have led to many changes in ecosystem functioning. Biological invasions can change species composition and interactions, and also the habitat structure in a system (Grosholz and Ruiz 2009). Increased fluxes of reactive nitrogen from nitrogen-fixing crops, fossil fuel combustion, and the Haber–Bosch process have led to increased anoxic and eutrophic conditions around the world (Seitzinger et al. 2006). Estuaries and coasts are hotspots for both species introductions and alterations to nutrient regimes. Nonnative species dispersal mechanisms such as ballast water exchange, ship fouling, aquaculture, and aquarium and food trade are all common in these systems (Grosholz and Ruiz 2009). Species introductions can change food web interactions, biodiversity, and nutrient dynamics (Grosholz and Ruiz 2009). Anthropogenic nutrient enrichment can also lead to shifts in primary producer communities, including dominance by phytoplankton or blooming ephemeral macroalgae (McGlathery et al. 2007), reductions in seagrass coverage (McGlathery 2001), increased anoxia, and reductions in benthic fauna (Karlson et al. 2002). To remediate these negative effects, managers often focus on increasing the nitrogen removal capacity of ecosystems (Seitzinger et al. 2006).

In coastal systems, many processes interact to affect retention and removal of nitrogen. Nitrogen can be lost from estuaries three ways: burial, physical transport, and denitrification, the microbially mediated reduction of nitrate to N_2 gas (Seitzinger et al. 2006). Nitrate for denitrification can come either directly from the surrounding environment (direct denitrification) or from coupling with nitrification (coupled nitrification–denitrification). Coupling, rather than direct denitrification, is more common in estuaries with low dissolved nutrients and good water quality (Seitzinger et al. 2006). Whereas denitrification requires anoxic conditions, nitrification requires aerobic conditions. Estuaries are dynamic environments where tidal fluctuations can create oxygenated conditions for nitrification at low tide, facilitating nitrate loss through denitrification after the sediments are inundated and reduced at high tide (Ensign et al. 2008). However, estuarine rates of denitrification can be increased if oxygen conditions in the sediments are more heterogeneous, with many oxic–anoxic interfaces for coupled denitrification (Eyre and Ferguson 2009). Systems in which anoxic conditions dominate will meet carbon and oxygen state requirements for denitrification but can be nitrate limited because of inhibition of nitrification (Joye and Hollibaugh 1995; Webster and Harris 2004; Eyre and Ferguson 2009). Conversely, entirely oxic conditions will have nitrate available from nitrification but will lack the anoxic conditions necessary for denitrification to proceed (Webster and Harris 2004; Eyre and Ferguson 2009).

To date, the evidence for an effect of macroalgal mats on denitrification is equivocal. Macroalgal mats can be associated with decreases in denitrification rates because of macroalgal competition with microbes for nitrate (Dalsgaard 2003). However, denitrification rates on macroalgal vegetated sediments can also be no different from those on bare sediments, either because of a shift in the oxic–anoxic boundary for coupled nitrification–denitrification into the macroalgal mat or because enough dissolved inorganic nitrogen (DIN) is available to satisfy both macroalgal growth and denitrification requirements (Krause-Jensen et al. 1999; Bartoli et al. 2012). Alternatively, recent work by Eyre et al. (2011*b*) has indicated that

* Corresponding author: djg4j@virginia.edu

biomass of the invasive macroalga, *Caulerpa taxifolia*, can be associated with increased rates of denitrification, most likely because the macroalgae oxygenate sediments around their rhizoids and thus increase oxic–anoxic hotspots for coupled nitrification–denitrification within the sediments. This relationship between root oxygenation and increased denitrification rates has been well documented for many marine macrophytes (Risgaard-Petersen and Jensen 1997). It is also possible that macroalgal presence could enhance carbon availability for denitrification by releasing between 1.1% and 40% of carbon fixed via photosynthesis (Khailov and Burlakova 1969; Brylinsky 1977).

The goal of this study was to determine how the introduction of the nonnative macroalga, *Gracilaria vermiculophylla,* affected net denitrification on a mid-Atlantic, U.S.A., intertidal mudflat. This macroalga is native to Southeast Asia and has been introduced to temperate estuaries around the world. It has been hypothesized that this introduction unintentionally occurred in the 1970s in the mid-Atlantic region via attachment to traded oysters (Thomsen et al. 2006; Gulbransen et al. 2012). It has been the dominant macroalgal species in the region since routine monitoring began in 1998, and recent seasonal surveys have documented biomasses on mudflats as high as 800 g dry weight (dry wt) m^{-2} (Gulbransen and McGlathery 2013). Rather than forming mats that only lie on the surface of the sediment, *G. vermiculophylla* thalli are often found incorporated several centimeters into the sediment (pers. obs.). Although prior work has shown that this macroalga can increase epifaunal densities on mudflats (Byers et al. 2012) and mediate transfers of nitrogen to higher trophic levels (Gulbransen and McGlathery 2013), little is known about how this introduction could be affecting sediment nitrogen dynamics on intertidal mudflats.

We hypothesized that *G. vermiculophylla* presence on intertidal mudflats would enhance rates of net denitrification compared with bare substrate by increasing oxic–anoxic hotspots for coupled nitrification–denitrification. We also hypothesized that at high densities, *G. vermiculophylla* coverage would be associated with highly reduced conditions that would inhibit nitrification and reduce overall coupled denitrification. To test these hypotheses, we collected microcosms with (vegetated) and without (bare) *G. vermiculophylla* biomass for continuous-flow incubations twice in the summer and once in the fall of 2012.

Methods

Study site—Samples were collected from an intertidal mudflat within the Virginia Coast Reserve Long Term Ecological Research (VCR LTER) site (37°18′20″N, 75°53′59″W). The coastal bays that make up the VCR LTER site span 110 km of coastline on the eastern shore of the Delmarva Peninsula and are enclosed by barrier islands to the east. The site has been minimally affected by humans, and water quality, as assessed using dissolved nutrient concentrations and chlorophyll *a* content, has remained stable for the last 20 yr (McGlathery et al. 2012).

Sample collection—Microcosm cores (6.4 cm diameter by ~ 17 cm sediment depth, ~ 400 mL of overlying water) were collected within 2 h of low tide on three dates. Two of these sample dates were in the summer: once when macroalgal coverage was moderate (11 June 2012) and once when coverage was much higher (23 July 2012). One additional fall sampling was conducted after much of the summer biomass had been removed by storm activity (28 September 2012).

At each collection time, four bare microcosms, with only mudflat sediment, and four vegetated microcosms, with *G. vermiculophylla* densities approximately equivalent to 40 g dry wt m^{-2}, were collected (Table 1). In July, an additional four cores were collected with more than twice as much *G. vermiculophylla* biomass as in the other vegetated cores.

Preliminary experiments showed that adding *G. vermiculophylla* onto collected bare sediments underestimated denitrification rates compared with sediments collected with *G. vermiculophylla* intact. Thus, vegetated cores were collected intact, with care taken not to disturb the algae–sediment interface. In addition to sediment microcosms, 190 L of water was collected from the channel adjacent to the mudflat for the continuous-flow incubations. Water column temperature, dissolved oxygen, and salinity were measured using a handheld Yellow Springs Instrument Model 556.

Continuous-flow incubation—Upon collection, water and microcosms were transported, in the dark, on ice, with water overlying the headspace, to the University of North Carolina Institute of Marine Sciences in Morehead City, North Carolina. Microcosms were submerged in an aerated water bath in an environmental chamber (Bally) at in situ temperatures in the dark for 12–16 h (Fulweiler and Nixon 2012). Each microcosm was capped with an air-tight Plexiglas top that was equipped with an inflow and outflow sampling port and incubated in a continuous-flow system. Dark conditions were maintained throughout the incubations because preliminary experiments showed that the use of light levels realistic for the study site caused photosynthesis-mediated bubble formation. Aerated and unfiltered water was passed over each microcosm at a flow rate of 1.5 mL min^{-1}, which created a well-mixed water column within the chamber. It is unlikely that macroalgal decomposition occurred over the course of this experiment. *G. vermiculophylla* is highly tolerant to fluctuations in light, temperature, nutrients, and salinity (e.g., Thomsen and McGlathery 2007); therefore, it is improbable that core incubations were extreme enough to cause algal death.

Microcosms were acclimated in the system for 24 h before sampling to allow the system to reach steady state (Eyre et al. 2002). Water samples (5 mL) were collected at 0, 8, and 24 h after the 24 h acclimation period to ensure steady-state conditions were reached with respect to O_2 concentrations in the outflow of each core. Inflow and outflow samples were collected at the same time. Inflow water (measured from a bypass line that flowed directly into sample vials) and outflow water leaving the microcosms were analyzed for N_2, O_2, and Ar dissolved gases in water using a Balzers Prisma QME 200 quadruple mass spectrometer (membrane inlet mass spectrometer [MIMS], Pfeiffer Vacuum; Kana et al. 1994). Concentrations of O_2 and N_2 were determined using the ratio with Ar (Kana

Table 1. Average *Gracilaria vermiculophylla* biomass, cumulative N_2-N fluxes, and biological oxygen demand (BOD), mean ± standard error (SE) for each sample date. Sample size (*n*) indicates the number of microcosms used for calculations. Only one core from the high-biomass set in July is reported here because all other cores had bubbles.

Date and coverage	Sample size (*n*)	*G. vermiculophylla* biomass (g dry wt m^{-2})	N_2-N flux (μmol m^{-2} h^{-1})	BOD (μmol m^{-2} h^{-1})
June bare	3	0	25.48±15.09	522.50±122.30
June vegetated	3	39.48±2.48	182.37±16.87	3460.50±382.17
July bare	3	0	254.81±19.86	2176.62±186.92
July vegetated	3	42.13±9.79	213.19±16.30	1718.77±364.72
July high biomass	1	122.41	70.76	1214.24
September bare	4	0	46.47±15.79	697.34±122.37
September vegetated	3	44.60±16.39	124.82±11.17	2053.40±312.11

et al. 1994; Ensign et al. 2008). We used the gas ratios with Ar rather than the gas concentrations alone to partition physical and biological effects on samples. Concentrations of N_2 gas in samples ($[N_{2samp}]$) were calculated as

$$[N_2]_{samp} = N_2:Ar_{samp} \times [Ar]_{std} \times \left\{ \frac{([N_2]:[Ar])_{std}}{(N_2:Ar)_{DI}} \right\}$$

where $N_2:Ar_{samp}$ was the signal measured in the sample and $(N_2:Ar)_{DI}$ was the signal measured in deionized water at the same temperature as samples. Gas solubility tables were used to determine $[Ar]_{std}$ and $([N_2]:[Ar])_{std}$ at in situ sample temperature and salinity.

The MIMS technique has a rapid analysis time, requires a small sample volume and little sample preparation and has high precision (coefficient of variation of $N_2:Ar < 0.05\%$). This method determines net N_2 fluxes such that a positive N_2 flux is attributed to net denitrification, whereas a negative N_2 flux is attributed to net nitrogen fixation. This method does not discern between the sources of N_2; therefore, net denitrification refers to N_2 production from heterotrophic denitrification, anaerobic ammonium oxidation (anammox), and any other N_2-producing process, regardless of its mechanism. Fluxes of oxygen directed into the sediment were considered to represent rates of biological oxygen demand (BOD; Kana et al. 1994; Piehler and Smyth 2011).

Replicate cores in which it was evident that an invertebrate in the core had died or bubble formation was an issue were not used in the analysis. It is well documented that bubble formation artificially reduces dissolved N_2 concentrations measured relative to Ar, because N_2 more readily diffuses into bubbles, thus reducing the dissolved concentrations within cores (Eyre et al. 2002). Therefore, for some sampling periods we had three rather than four replicate cores within each bare and vegetated treatment (Table 1). Additionally, bubble formation occurred in three of the high-biomass cores in July, most likely from CH_4 release from the sediments. Therefore, only gas fluxes from one core with the equivalent 122 g dry wt m^{-2} of *G. vermiculophylla* were used, but all four cores were used for nutrient fluxes and sediment carbon and nitrogen content.

Nutrients—Water samples (50 mL) were collected for nutrient analysis from the bypass line and the outflow port of each core once during the incubation after steady-state conditions were reached. Water was filtered through Whatman GF/F filters (25 mm diameter, 0.7 μm nominal pore size), and the filtrate was analyzed with a Lachat Quick-Chem 8500 (Lachat Instruments) automated ion analyzer for nitrate (NO_3^- and NO_2^-, NO_x in remainder of paper), ammonium (NH_4^+), phosphate (PO_4^{3+}), and total dissolved nitrogen (TDN). Lower detection limits for ammonium, nitrate, and TDN were 0.36 μmol L^{-1}, whereas the detection limit for phosphate was 0.16 μmol L^{-1}. Dissolved organic nitrogen (DON) was calculated by subtracting NH_4^+ and NO_x from TDN.

At the end of each experiment, sediment samples from the upper 2 cm of sediment within each microcosm were collected, dried, and ground for C : N analysis using a Carlo Erba elemental analyzer. *G. vermiculophylla* within each vegetated core were rinsed with distilled (DI) water, dried in a 60°C oven for 48 h, and weighed.

Flux calculations—Flux calculations determined in the dark incubations were based on the assumption of steady-state conditions and a homogeneous water column (Miller-Way and Twilley 1996).

Briefly, fluxes of dissolved nutrients and gasses (J) were calculated using

$$J = ([i_{outflow}] - [i_{inflow}]) \times \frac{F}{A}$$

where $[i_{outflow}]$ and $[i_{inflow}]$ are the concentrations (μmol L^{-1}) of dissolved gases or nutrients leaving and entering each core; F is the flow rate (L h^{-1}); and A is the core surface area (m^2; Miller-Way and Twilley 1996). A positive flux, which occurred when outflow water had higher gas or nutrient concentrations, or both, than inflow water, indicated production within the microcosm, whereas a negative flux, which occurred when outflow water had lower concentrations than inflow water, indicated uptake within the microcosm.

Although isotope pairing is often used to measure coupled nitrification–denitrification and anammox directly (Eyre et al. 2002), this technique can be prohibitively expensive in a flow-through system. Therefore, we used mass balance equations to estimate the percentage of denitrification that was likely coupled to nitrification (Groffman et al. 2006; Fennel et al. 2009) as

$$DNF_C = DNF_T + x$$

Table 2. In situ water properties at each sampling date. DO, dissolved oxygen; na, data not available.

Date	Temperature (°C)	Salinity	DO (mg L^{-1})	DO (MIMS)	NO_x (μmol L^{-1})	NH_4^+ (μmol L^{-1})	PO_4^{3+} (μmol L^{-1})
11 Jun	25	32	8.9	5.3	0	0	0
23 Jul	27	31	na	2.8	0.24	0	0.05
28 Sep	22	33	7.16	6.2	0.70	0.48	0.34

where DNF_C is coupled nitrification–denitrification, DNF_T is the total N-N_2 efflux, and x is the measured nitrate flux. Only negative nitrate fluxes were used for this calculation; if the nitrate flux was positive, we assumed that all denitrification was coupled. This method assumes nitrogen fixation and anammox are minimal.

Data analysis—Net fluxes of N_2, O_2, ammonium, nitrate, phosphate, and DON for each sample period on bare and vegetated areas were compared using *t*-tests in SAS 9.2 (SAS Institute). All data met assumptions and were not transformed. Significant Pearson correlations (r) between all fluxes, *G. vermiculophylla* biomass, and sediment nitrogen and carbon within each core were calculated in SAS. Calculations for high-biomass cores in July were analyzed separately from July cores with average vegetation densities.

Results

Water chemistry and algal biomass—Water temperature was highest in July (27°C), and salinity ranged from 31 to 33 (Table 2). Dissolved oxygen (DO) in the reservoir water ranged from 2.8 mg L^{-1} in July to 6.2 mg L^{-1} in September. Nitrate, ammonium, and phosphate were below detection in June and July and only slightly above detection limits in September (Table 2). *G. vermiculophylla* biomass within microcosms was near 40 g dry wt m^{-2} in all incubations (Table 1).

N_2 fluxes—Net N_2 fluxes were significantly higher (more positive) in *G. vermiculophylla*–covered areas in June (p = 0.0023) and September (p = 0.0133), but not in July (p = 0.1806; Fig. 1). Lowest net denitrification was recorded on bare sediments in June (25.48 μmol m^{-2} h^{-1}; Table 1). Highest N_2 production occurred in July on both bare (254.81 μmol m^{-2} h^{-1}) and vegetated substrates (213.19 μmol m^{-2} h^{-1}; Table 1). N_2 fluxes had strong positive correlations with *G. vermiculophylla* biomass in June (r = 0.98, p = 0.0007) and September (r = 0.79, p = 0.0359). The July high-biomass microcosm (122 g dry wt m^{-2} of *G. vermiculophylla*) had a net N_2 flux of 70.76 μmol m^{-2} h^{-1}.

Biological oxygen demand—BOD was significantly higher in *G. vermiculophylla* microcosms compared with bare mudflat sediments in June (p = 0.0019) and September (p = 0.0062), but not significantly different in July (p = 0.3265; Fig. 1). The lowest measured BOD was found in bare microcosms in June (522.50 μmol m^{-2} h^{-1}), and the highest was measured in the same month in microcosms with *G. vermiculophylla* biomass (3460.50 μmol m^{-2} h^{-1}; Table 1). BOD had a strong, significant, positive correlation to N_2 fluxes in June (r = 0.98, p = 0.0007), July (r = 0.86, p = 0.0297), and September (r = 0.95, p = 0.0009). The July high-biomass microcosm (122 g dry wt m^{-2} of *G. vermiculophylla*) had a BOD of 1214.24 μmol m^{-2} h^{-1}.

Nutrient fluxes—Nitrate fluxes were always the same in bare and vegetated microcosms and were either undetectable in June or negative in July and September (Fig. 2, Table 3). Ammonium fluxes were undetectable in July and negative but not significantly different between bare and vegetated microcosms in September (p = 0.7175). In June, vegetated cores produced ammonium when compared with the negligible flux in bare microcosms, but this difference was not significant (p = 0.0715; Table 3). Although phosphate fluxes were higher in vegetated cores in both June and July, these differences were only significant in July (p = 0.1501 and 0.0033, respectively; Table 3). Phosphate fluxes in September were always negative and were not significantly different from one another (p = 0.3524). DON fluxes were positive in all incubations (Fig. 2, Table 3). However, only in July were DON fluxes significantly higher in vegetated cores (p = 0.0138). The July high-biomass microcosms had no nitrate flux but did have high ammonium (814.91 ± 280.41), DON (1758.36 ± 1046.56), and phosphate (47.28 ± 32.52) fluxes.

On the basis of mass balance calculations, all denitrification in bare and vegetated microcosms in June was coupled to nitrification. In July, 95–100% of denitrification was estimated to have been coupled to nitrification in all microcosms. In contrast, in September, we estimated that coupled nitrification–denitrification accounted for 0–77% of denitrification in bare microcosms and 82–86% of denitrification in vegetated microcosms.

Sediment carbon and nitrogen—Both carbon and nitrogen content in sediments were highest in July microcosms when bare cores and cores with average amounts of vegetation were compared among dates (Table 4). Within each sample date, sediment percent carbon was significantly higher in *G. vermiculophylla*–vegetated microcosms in June (p = 0.0059), July (p = 0.0007), and September (p = 0.0030). Additionally, sediment percent nitrogen content was significantly higher when *G. vermiculophylla* was present in June (p = 0.0073), July (p = 0.0007), and September (p = 0.0021). Although there was a positive correlation between *G. vermiculophylla* biomass and sediment percent carbon and nitrogen content during all sample periods, the correlations were only significant in June (C: r = 0.90, p = 0.0141; N: r = 0.90, p = 0.0159) and

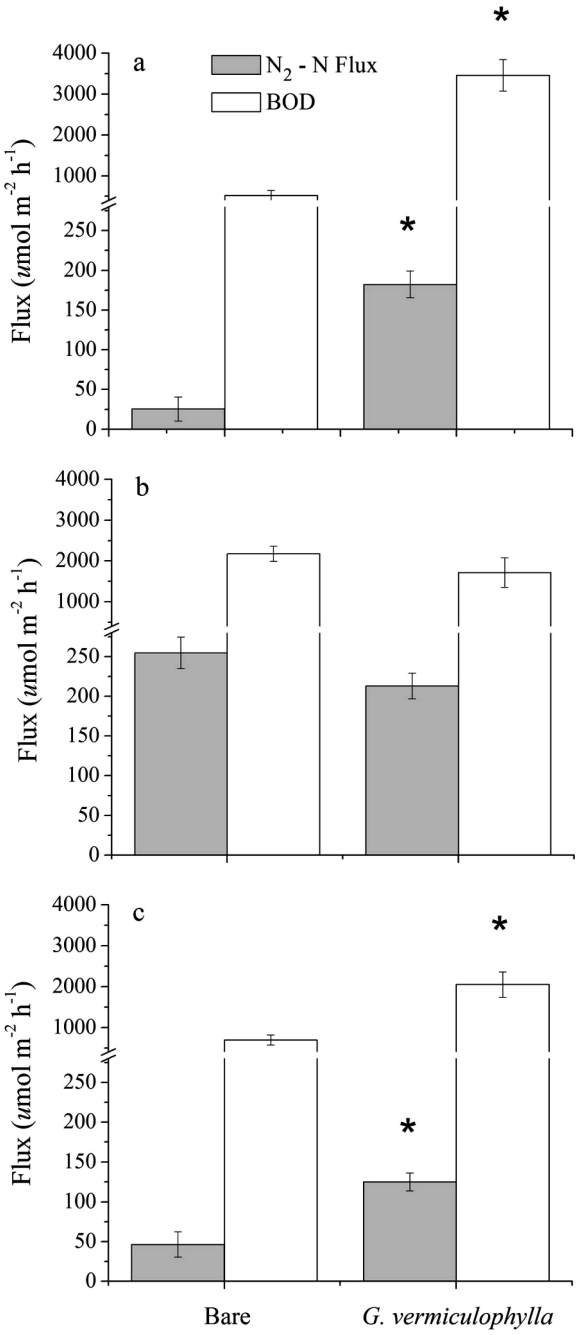

Fig. 1. Cumulative N_2-N flux and biological oxygen demand (BOD) for (a) June, (b) July, and (c) September incubations. An asterisk indicates a significant difference between N_2-N fluxes or BOD individually.

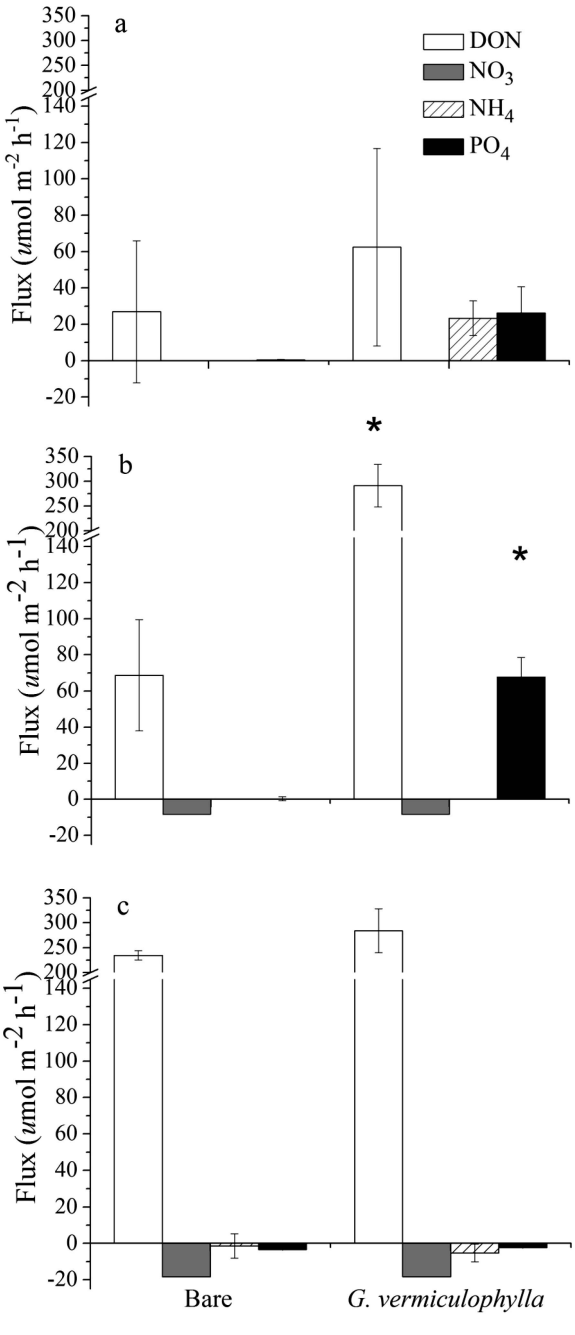

Fig. 2. Dissolved organic nitrogen (DON), nitrate (NO_3^-), ammonium (NH_4^+), and phosphate (PO_4^{3+}) fluxes for (a) June, (b) July, and (c) September incubations. An asterisk indicates a significant difference between fluxes from bare and *Gracilaria vermiculophylla*–vegetated microcosms.

July (C: $r = 0.87$, $p = 0.0213$; N: $r = 0.87$, $p = 0.0242$). Sediment percent carbon (2.36%) and percent nitrogen (0.25%) were highest in the July high-biomass microcosms.

Discussion

N_2 fluxes—The increased net denitrification in June and September was likely attributable to increased carbon availability and increased habitat heterogeneity associated with the algal biomass (Table 4; Eyre and Ferguson 2009; Eyre et al. 2011*b*). In July, however, net denitrification was not significantly different in bare and vegetated cores. During this time the sediments also had the highest carbon content measured in all of the incubations. Therefore, it is possible that increased metabolism in summer, either from phytoplankton or benthic microalgae (McGlathery et al. 2001), led to increased production of high-quality organic matter on both bare and vegetated substrates, which in turn led to high rates of denitrification everywhere. The slight

Table 3. Dissolved organic nitrogen (DON), NO_x, NH_4^+, and PO_4^{3+} fluxes at each sample date (all ± SE). All four July high-biomass cores were included here because bubble formation should not have altered nutrient fluxes.

	Flux (μmol m^{-2} h^{-1})			
Date and coverage	DON	NO_x	NH_4^+	PO_4^{3+}
June bare	26.87±39.09	0	0	0.41±0.36
June vegetated	62.41±54.34	0	23.33±9.58	26.23±14.52
July bare	68.70±30.78	−8.24±0	0	0.34±1.17
July vegetated	291.24±43.27	−8.24±0	0	67.77±10.70
July high biomass	1758.36±1046.56	0	814.91±280.41	47.28±32.52
September bare	234.42±9.35	−18.30±0	−1.36±6.69	−3.35±0.79
September vegetated	383.88±44.28	−18.30±0	−5.21±4.90	−2.26±0.60

drop in net denitrification in vegetated microcosms compared with bare microcosms could be attributed to reduced conditions, as supported by the phosphate efflux (Eyre et al. 2011*b*). These reduced conditions could limit nitrification and thus reduce net denitrification (Joye and Hollibaugh 1995; Webster and Harris 2004; Eyre and Ferguson 2009).

The system seemed to exhibit subsidy–stress characteristics, as described in Odum et al. (1979), with macroalgal density acting as the perturbation. As such, it appeared that once macroalgal biomass increased beyond a certain threshold, denitrification was inhibited by homogeneous, anoxic conditions that reduce nitrification. Lower rates of net denitrification within the high-biomass microcosm in July (122 g dry wt m^{-2} *G. vermiculophylla*) and increased phosphate and ammonium fluxes from all high-biomass microcosms, provide limited evidence to support this hypothesis. Future research should further test this hypothesis by increasing replication of high-biomass microcosms.

Net denitrification rates from vegetated microcosms in this experiment were on the upper end of rates seen in other studies with macrophytes, in particular macroalgae. Although some of the comparison studies incorporated light incubations into their studies (Dalsgaard 2003; Eyre et al. 2011*a*,*b*; Bartoli et al. 2012), we focused on fluxes measured under dark conditions. Additionally, all but two studies (Piehler and Smyth 2011; Smyth et al. 2013) used batch core incubations, and three of the studies used isotope pairing to separate direct and coupled denitrification (Krause-Jensen et al. 1999; Dalsgaard 2003; Bartoli et al. 2012). When compared with fluxes measured in seagrass beds, our rates were much higher than those measured annually in sediments vegetated with *Halophila ovalis* and *Halophila spinulosa* in Australia (77–109 μmol m^{-2} h^{-1}, Eyre et al. 2011*a*) and *Zostera capricorni* in Australia in summer (average < 50 μmol m^{-2} h^{-1}, Eyre et al. 2011*b*) but were similar to fluxes seen in mixed beds of *Halodule wrightii* and *Zostera marina* in North Carolina (< 200 μmol m^{-2} h^{-1} in each season, Piehler and Smyth 2011; Smyth et al. 2013) and lower than winter fluxes measured in winter *Z. capricorni* beds in Australia (412 μmol m^{-2} h^{-1}, Eyre et al. 2011*a*). All prior studies on denitrification fluxes with macroalgal presence have found lower rates of denitrification that range from almost zero up to 55 μmol m^{-2} h^{-1} (Dalsgaard 2003; Eyre et al. 2011*b*; Bartoli et al. 2012). Because our incubations were done in the dark, it is likely that competition for available nitrogen between macroalgae and denitrifying bacteria was reduced, and therefore net denitrification rates were higher. Of previous macroalgal studies, only one specifically used macroalgae that protruded into the sediments (Eyre et al. 2011*b*); all others used macroalgae lying on top of sediments (Krause-Jensen et al. 1999; Dalsgaard 2003; Bartoli et al. 2012). It is possible that by protruding 5 to 10 cm into the sediments, *G. vermiculophylla* may have increased oxygen heterogeneity in the sediments and led to more oxic–anoxic microzones for coupled nitrification–denitrification. This interpretation is supported by our mass balance calculations that estimate that 80% of denitrification was coupled to nitrification in vegetated cores during all sampling periods. Although we do not have sediment oxygen profiles, there was an uptake of O_2 in the dark, which may have been used to support nitrification. Additionally, nutrient fluxes in June and September do not indicate highly reduced conditions during incubations. A similar finding was reported by Joye et al. (2003), where cores left in the dark for 6 d did not appear to be anoxic on the basis of nutrient fluxes until 2 to 3 d of incubation.

Table 4. Sediment percent nitrogen and percent carbon content in bare and vegetated microcosms for all sampling dates (mean ± SE). Sample size (*n*) indicates the number of microcosms. Significant differences ($p < 0.05$) between treatment (bare, vegetated, high) nitrogen and carbon content are indicated with asterisks (*). Comparisons were made within each sample period (i.e., June, July, or September).

Date and coverage	*n*	Sediment C (%)	Sediment N (%)
June bare	3	0.92±0.04	0.07±0.004
June vegetated	3	1.55±0.11*	0.13±0.01*
July bare	3	1.14±0.06	0.09±0.01
July vegetated	3	1.68±0.01*	0.16±0.002*
July high biomass	4	2.36±0.12**	0.25±0.02**
September bare	4	1.04±0.01	0.08±0.001
September vegetated	3	1.30±0.05*	0.11±0.005*

Biological oxygen demand—All of the incubations showed a strong positive relationship between BOD and net N_2 flux, further supporting prior assertions that oxygen demand can be used to predict denitrification in systems (Fennel et al. 2009; Piehler and Smyth 2011). In June and

September, BOD was positively correlated to *G. vermiculophylla* biomass under dark incubation conditions, which indicated that, at higher *G. vermiculophylla* biomasses, an active microbial community was breaking down organic matter, with more reduced conditions that enhanced net denitrification rates (Piehler and Smyth 2011). The relationship between BOD and *G. vermiculophylla* biomass was negative, but not significant in July, which might indicate that all microcosms had highly active microbial communities and similarly favorable conditions for denitrification, as suggested by a lack of differences between net N_2 fluxes. This conclusion is also supported by high C and N levels found in the sediments in both bare and vegetated microcosms.

Summary and future—Current densities of *G. vermiculophylla* on Virginia coastal bay mudflats vary greatly in space and time from negligible amounts to biomasses as high as 800 g dry wt m^{-2} at some sites in warmer months (Gulbransen and McGlathery 2013). In this study, we found that at moderate densities (~40 g dry wt m^{-2}), *G. vermiculophylla* biomass enhanced net denitrification from mudflat communities. However, preliminary data from one microcosm incubation suggest that the system may fit the subsidy–stress model described in Odum et al. (1979), with a threshold density of *G. vermiculophylla* above which net denitrification was inhibited. Therefore, it is important to note that under a higher nutrient-loading regime in the Virginia coastal bays, variable outcomes are possible. We would likely see increased *G. vermiculophylla* biomass on mudflats, which would lead to a more anoxic, homogeneous environment not conducive to coupled nitrification–denitrification.

Future work should investigate how *G. vermiculophylla* moves in space and time and what factors lead to dense mat formation. Additionally, isotope pairing in a batch core setup should be conducted to provide a more mechanistic understanding of the differences in bare and *G. vermiculophylla*–vegetated areas under both light and dark conditions. In this study, we incubated cores at three distinct time periods. Although this design gave insight into how *G. vermiculophylla* affected nitrogen fluxes during these sample periods, our results cannot be extrapolated to all field conditions. Additional core incubations with more variations of *G. vermiculophylla* biomass, especially at high densities, and at more time points will be needed before determination of potential biomass thresholds will be possible.

Acknowledgments

Thank you to Raul Gonzalez, Meg Miller, and Suzanne Thompson for lab and statistical support. We also thank J. Thad Scott and an additional anonymous reviewer for their helpful comments. Funding for this work was provided by the Virginia Coast Reserve Long Term Ecological Research Grant Division of Environmental Biology-0621014.

References

Bartoli, M., G. Castaldelli, D. Nizzoli, and P. Viaroli. 2012. Benthic primary production and bacterial denitrification in a Mediterranean eutrophic coastal lagoon. J. Exp. Mar. Biol. Ecol. **438:** 41–51, doi:10.1016/j.jembe.2012.09.011

Brylinsky, M. 1977. Release of dissolved organic matter by some marine macrophytes. Mar. Biol. **39:** 213–220, doi:10.1007/BF00390995

Byers, J. E., P. E. Gribben, C. Yeager, and E. E. Sotka. 2012. Impacts of an abundant introduced ecosystem engineer within mudflats of the southeastern US coast. Biol. Invasions **14:** 2587–2600, doi:10.1007/s10530-012-0254-5

Dalsgaard, T. 2003. Benthic primary production and nutrient cycling in sediments with benthic microalgae and transient accumulation of macroalgae. Limnol. Oceanogr. **48:** 2138–2150, doi:10.4319/lo.2003.48.6.2138

Ensign, S. H., M. F. Piehler, and M. W. Doyle. 2008. Riparian zone denitrification affects nitrogen flux through a tidal freshwater river. Biogeochemistry **91:** 133–150, doi:10.1007/s10533-008-9265-9

Eyre, B. D., and A. J. P. Ferguson. 2009. Denitrification efficiency for defining critical loads of carbon in shallow coastal ecosystems. Hydrobiologia **629:** 137–146, doi:10.1007/s10750-009-9765-1

———, ———, A. Webb, D. Maher, and J. M. Oakes. 2011*a*. Denitrification, N-fixation and nitrogen and phosphorus fluxes in different benthic habitats and their contribution to the nitrogen and phosphorus budgets of a shallow oligotrophic sub-tropical coastal system (southern Moreton Bay, Australia). Biogeochemistry **102:** 111–133, doi:10.1007/s10533-010-9425-6

———, D. Maher, J. M. Oakes, D. V. Erler, and T. M. Glasby. 2011*b*. Differences in benthic metabolism, nutrient fluxes, and denitrification in *Caulerpa taxifolia* communities compared to uninvaded bare sediment and seagrass (*Zostera capricorni*) habitats. Limnol. Oceanogr. **56:** 1737–1750.

———, S. Rysgaard, T. Dalsgaard, and P. B. Christensen. 2002. Comparison of isotope paring and N_2 : Ar methods for measuring sediment denitrification—assumptions, modifications, and implications. Estuaries **25:** 1077–1087, doi:10.1007/BF02692205

Fennel, K., and others. 2009. Modeling denitrification in aquatic sediments. Biogeochemistry **93:** 159–178, doi:10.1007/s10533-008-9270-z

Fulweiler, R. W., and S. W. Nixon. 2012. Net sediment N_2 fluxes in a southern New England estuary: Variations in space and time. Biogeochemistry **111:** 111–124, doi:10.1007/s10533-011-9660-5

Groffman, P. M., and others. 2006. Methods for measuring denitrification: Diverse approaches to a difficult problem. Ecol. Appl. **16:** 2091–2122, doi:10.1890/1051-0761(2006)016[2091:MFMDDA]2.0.CO;2

Grosholz, E. D., and G. M. Ruiz. 2009. Multitrophic effects of invasions in marine and estuarine systems, p. 305–324. *In* G. Rilov and J. A. Crooks [eds.], Biological invasions in marine ecosystems. Springer-Verlag.

Gulbransen, D. J., and K. J. McGlathery. 2013. Nitrogen transfers mediated by a perennial, non-native macroalga: A ^{15}N tracer study. Mar. Ecol. Prog. Ser. **482:** 299–304, doi:10.3354/meps10289

———, ———, M. Marklund, J. N. Norris, and C. F. D. Gurgel. 2012. *Gracilaria vermiculophylla* (Rhodophyta, Gracilariales) in the Virginia coastal bays, USA: *Cox*1 analysis reveals high genetic richness of an introduced macroalga. J. Phycol. **48:** 1278–1283, doi:10.1111/j.1529-8817.2012.01218.x

Joye, S. B., and J. T. Hollibaugh. 1995. Influence of sulfide inhibition of nitrification on nitrogen regeneration in sediments. Science **270:** 623–625, doi:10.1126/science.270.5236.623

———, W. Porubsky, N. Weston, and R. Lee. 2003. Benthic microalgal production and nutrient dynamics in intertidal sediments. Ber. FZKA **12:** 67–70.

Kana, T. M., C. Darkangelo, M. D. Hunt, J. B. Oldham, G. E. Bennett, and J. C. Cornwell. 1994. Membrane inlet mass spectrometer for rapid high-precision determination of N_2, O_2, and Ar in environmental water samples. Anal. Chem. **66:** 4166–4170, doi:10.1021/ac00095a009

Karlson, K., R. Rosenberg, and E. Bonsdorff. 2002. Temporal and spatial large-scale effects of eutrophication and oxygen deficiency on benthic fauna in Scandinavian and Baltic waters: A review. Oceanogr. Mar. Biol. **40:** 427–489.

Khailov, W. M., and Z. P. Burlakova. 1969. Release of dissolved organic matter from seaweeds and distribution of their total organic production in inshore communities. Limnol. Oceanogr. **14:** 521–527, doi:10.4319/lo.1969.14.4.0521

Krause-Jensen, D., P. B. Christensen, and S. Rysgaard. 1999. Oxygen and nutrient dynamics within mats of the filamentous macroalga *Chaetomorpha linum*. Estuaries **22:** 31–38, doi:10.2307/1352924

McGlathery, K. J. 2001. Macroalgal blooms contribute to the decline of seagrass in nutrient-enriched coastal waters. J. Phycol. **37:** 453–456, doi:10.1046/j.1529-8817.2001.037004453.x

———, I. C. Anderson, and A. C. Tyler. 2001. Magnitude and variability of benthic and pelagic metabolism in a temperate coastal lagoon. Mar. Ecol. Prog. Ser. **216:** 1–15, doi:10.3354/meps216001

———, L. K. Reynolds, L. W. Cole, R. J. Orth, S. R. Marion, and A. Schwarzschild. 2012. Recovery trajectories during state change from bare sediment to eelgrass dominance. Mar. Ecol. Prog. Ser. **448:** 209–221, doi:10.3354/meps09574

———, K. Sundback, and I. C. Anderson. 2007. Eutrophication in shallow coastal bays and lagoons: The role of plants in the coastal filter. Mar. Ecol. Prog. Ser. **348:** 1–18, doi:10.3354/meps07132

Miller-Way, T., and R. R. Twilley. 1996. Theory and operation of continuous flow systems for the study of benthic–pelagic coupling. Mar. Ecol. Prog. Ser. **140:** 257–269, doi:10.3354/meps140257

Odum, E. P., J. T. Finn, and E. H. Franz. 1979. Perturbation theory and the subsidy–stress gradient. BioScience **29:** 349–352, doi:10.2307/1307690

Piehler, M. F., and A. R. Smyth. 2011. Habitat-specific distinctions in estuarine denitrification affect both ecosystem function and services. Ecosphere **2:** 1–16, doi:10.1890/ES10-00082.1

Risgaard-Petersen, N., and K. Jensen. 1997. Nitrification and denitrification in the rhizosphere of the aquatic macrophyte *Lobelia dortmanna* L. Limnol. Oceanogr. **42:** 529–537.

Seitzinger, S., J. A. Harrison, J. K. Böhlke, A. F. Bouwman, R. Lowrance, B. Peterson, C. Tobias, and G. Van Drecht. 2006. Denitrification across landscapes and waterscapes: A synthesis. Ecol. Appl. **16:** 2064–2090, doi:10.1890/1051-0761(2006)016[2064:DALAWA]2.0.CO;2

Smyth, A. R., S. P. Thompson, K. N. Siporin, W. S. Gardner, M. J. McCarthy, and M. F. Piehler. 2013. Assessing nitrogen dynamics throughout the estuarine landscapes. Estuar. Coasts **36:** 44–55, doi:10.1007/s12237-012-9554-3

Thomsen, M. S., C. F. D. Gurgel, S. Fredericq, and K. J. McGlathery. 2006. *Gracilaria vermiculophylla* (Rhodophyta, Gracilariales) in Hog Island Bay, Virginia: A cryptic alien and invasive macroalga and taxonomic correction. J. Phycol. **42:** 139–141, doi:10.1111/j.1529-8817.2006.00160.x

———, and K. J. McGlathery. 2007. Stress tolerance of the invasive macroalgae *Codium fragile* and *Gracilaria vermiculophylla* in a soft-bottom turbid lagoon. Biol. Invasions **9:** 499–513, doi:10.1007/s10530-006-9043-3

Webster, I. T., and G. P. Harris. 2004. Anthropogenic impacts on the ecosystems of coastal lagoons: Modeling fundamental biogeochemical processes and management implications. Mar. Freshw. Res. **55:** 67–78, doi:10.1071/MF03068

Associate editor: Anthony W.D. Larkum

Received: 05 March 2013
Accepted: 29 July 2013
Amended: 30 July 2013